



Particle swarm optimization based design of a terahertz antenna with a modified photonic band gap substrate for 6G future wireless communications

6G geleceğin kablosuz iletişimi için modifiye fotonik bant boşluğu substratına sahip bir terahertz antenin parçacık sürü optimizasyonu temelli tasarımı

Tayfun Okan¹ , Seda Habergötüren Ateş^{2*} , Nursel Akçam³ 

^{1,2,3} Gazi University, Engineering Faculty, Electrical and Electronics Engineering Department, 06570, Maltepe/Ankara/Turkey

¹ Turkish Aerospace, 06980, Ankara/Turkey

Abstract

In this study, an antenna is proposed that operates at THz spectrum for sixth generation (6G) short-range future wireless communications. A modified photonic band gap (MPBG) substrate is employed to design an octagonal ring shaped microstrip patch antenna with wideband and high gain properties. Unlike the conventional photonic band gap (PBG) form, the proposed MPBG substrate structure is created by variable sized cylindrical air holes. The radii of each air cylinder in the row is determined with the help of particle swarm optimization (PSO) algorithm, where the goal is set to achieve the highest gain and impedance bandwidth ($S_{11} \leq -10$ dB) possible. The simulation results of the antennas that are built on 1) non-PBG, 2) conventional PBG and 3) the proposed MPBG substrate structures are compared. It is observed that the radiation performance is most enhanced by implementing MPBG structure. In comparison to the antenna without PBG, the reported MPBG structure offers almost 300% gain and 11% bandwidth improvement. To summarize, the designed antenna with its proposed MPBG substrate structure achieves an excellent radiation performance within a wide operating bandwidth.

Keywords: Terahertz antenna, Sixth generation (6G), Photonic band gap, Defective photonic crystal substrate, Particle swarm optimization

1 Introduction

Terahertz (THz) frequency band (0.1-10 THz) is taken into consideration by researchers; since there is an increasing demand to high data rate and wideband properties [1, 2]. As a result, THz antenna designs have been used in many various fields including imaging [3,4], biomedical applications [5-7], near field communications [8-11], wireless body area networks [12], vehicular communications [13] and future wireless communication [14-18]. Besides all advantages, the major drawback of these antennas is that they commonly exhibit short range wireless communications due to their high attenuated signal characteristic. Although, the THz spectrum has not yet been officially allocated by the competent authorities; in 2019, the Federal Communications Commission (FCC) has opened up 4 different unlicensed

Öz

Bu çalışmada, altıncı nesil (6G) kısa menzilli geleceğin kablosuz iletişimi için THz spektrumunda çalışan bir anten önerilmiştir. Geniş bant ve yüksek kazanç özelliklerine sahip sekizgen halka şeklinde bir mikroşerit yama anteni tasarlamak için değiştirilmiş bir fotonik bant aralığı (MPBG) kullanılır. Geleneksel fotonik bant aralığı (PBG) formunun aksine, önerilen MPBG substrat yapısı, değişken boyutlu silindirik hava delikleri tarafından oluşturulur. Sıradaki her hava silindirinin yarıçapı, hedefin mümkün olan en yüksek kazanç ve empedans bant genişliğini ($S_{11} \leq -10$ dB) elde etmek olan parçacık sürü optimizasyonu (PSO) algoritması yardımıyla belirlenir. 1) PBG olmayan, 2) geleneksel PBG ve 3) önerilen MPBG substrat yapıları üzerine kurulan antenlerin simülasyon sonuçları karşılaştırılmıştır. Radyasyon performansının en çok MPBG yapısının uygulanmasıyla arttığı gözlemlenmiştir. PBG'siz antenle karşılaştırıldığında, bildirilen MPBG yapısı neredeyse %300 kazanç ve %11 bant genişliği iyileştirmesi sunuyor. Özetlemek gerekirse, önerilen MPBG substrat yapısı ile tasarlanan anten, geniş bir çalışma bant genişliği içinde mükemmel bir radyasyon performansı elde etmektedir.

Anahtar Kelimeler: Terahertz anten, Altıncı nesil (6G), Fotonik bant aralığı, Kusurlu fotonik kristal substrat, Parçacık sürüsü optimizasyonu

bands, between 95 GHz to 3 THz, to be used for experimental 6G communication studies [19].

Microstrip antennas are frequently preferred in all frequency bands thanks to their low cost, low profile, easy to manufacture form [13]. In [14], four arm windmills shaped fractal microstrip antenna is designed. The presented antenna has a very compact size and wide operating frequency band. On the other hand, it does not include the sub-THz band. A high efficiency wideband microstrip patch antenna is reported in [15]. This antenna is printed on FR-4 substrate material, which is not a highly preferred material due to its performance at high frequencies. Another microstrip THz antenna is studied in [16] where radiation properties are improved with the help of a shorting pin. To overcome low gain, 12 element microstrip array antenna is designed in [17]

* Sorumlu yazar / Corresponding author, e-posta / e-mail: sedahabergoturen@gazi.edu.tr (S. H. Ates)
Geliş / Recieved: 10.12.2022 Kabul / Accepted: 20.03.2023 Yayınlanma / Published: 15.04.2023
doi: 10.28948/ngumuh.1217148

and particle swarm optimization method is utilized for microstrip patch antenna that has a partial ground plane in [18].

All the above mentioned microstrip THz antenna studies put forth a different design and dielectric material that the antenna is printed on. However, overall antenna performance improvements are not satisfactory. For example, if the bandwidth increases, the gain or efficiency value decreases. In summary, a trade-off situation exists. Therefore, different methods and structures are employed to enhance the bandwidth, gain and efficiency of antennas all at the same time. Defective photonic crystal substrate is one of the most efficient techniques used for this purpose. Even though, this structure is named differently within the studies as photonic band gap (PBG), modified photonic crystal or defective photonic crystal substrate; they all express the same substrate structure. A trapezoidal shaped microstrip THz antenna is designed in [20] and a surrounding PBG substrate framework is developed instead of periodic PBG for better performance outputs. In [21], bandwidth and gain properties of the reported antenna is enhanced by introducing a defected ground structure beside PBG. Particle swarm optimization algorithm is used in [22] to determine the optimum structure of PBG substrate. A PBG antenna with quadratic holes is investigated in [23] and the effect of the distance between air gaps is analyzed in [24]. Many of the THz antenna studies [25, 26] are analyzed at frequencies lower than 1 THz due to their high computational complexity. THz antennas that have periodic air cylinders embedded substrates are reported in many other studies [27-29] as well. To the best of authors' knowledge, only in [30] and [31], PBG substrates are realized with different sized aperiodic air cylinders. Radiation performances are further improved in these studies in comparison to conventional PBG THz antennas. However, the simulated results are performed only for a small frequency interval below 1 THz, and no algorithm or optimization is included to obtain the optimum size of air cylinders.

It is seen from the early studies that PBG substrates limit the effect of surface leaky waves beneath the patch. This helps to achieve noticeable improvement in radiation characteristics. Different from conventional photonic crystal substrates, a modified defective photonic crystal substrate is developed and employed in this study to reach the most successful simulation results possible. The proposed octagonal ring shaped microstrip patch antenna, with its aforementioned substrate structure, exhibits high impedance bandwidth, gain and efficiency results within the 0-2 THz frequency interval.

2 Antenna configuration

The main focus of this study is to present a THz antenna with a wideband and high gain property that can be used for 6G wireless communication systems. At first, a simple planar microstrip antenna is designed and it is evolved by modifying its conducting parts with time. PBG substrate is implemented afterwards and it is modified to further improve the radiation characteristics. Design process is started by determining the dielectric material that the antenna is printed

on. Rogers RO4350B is used as substrate material with a thickness of 64 μm . It has a permittivity of 3.66 and a loss tangent of 0.0037.

Copper is preferred as a conductor in this THz study. The reason it is used instead of any other material is that copper is suitable to be used for every low, medium and high voltage power network [32]. It is also very efficient thanks to its high conductivity value and it can be soldered with ease for durable connections. Graphene is employed as a conductor in some of the recent THz antenna studies [33-37]. Conductivity value of this material can be varied by changing its chemical potential. However, it is analyzed that antennas using copper as their conducting parts have higher gain values in comparison to antennas that use graphene as a conductor [32]. Hence the reason why graphene is not used in this study.

The proposed antenna design is depicted in Fig. 1. Grey parts represent copper that has a thickness of 18 μm and white sections represent the dielectric substrate material. An octagonal ring shaped radiator is excited by a trapezoidal microstrip feeding line. The antenna element is shifted by 100 μm (O) and the length of partial ground plane is 320 μm (L_g). A modified photonic band gap (MPBG) substrate structure is developed and implemented in this study, where defective photonic crystal substrate is created by drilling 6×6 holes. The diameters of the air cylinders in the first row of the substrate are determined as D_1, D_2, D_3, D_4, D_5 and D_6 , respectively. As seen in Fig. 1, these drilled holes are shifted to right one at a time in each row. The last hole in the row is shifted to the beginning in the next row. It is observed that using such a dynamic MPBG structure improves the performance of the antenna in comparison to conventional periodic PBG. Optimum diameter values of the air cylinders are specifically determined with the help of PSO algorithm [38]. PSO algorithm is an optimization technique available in CST Microwave Studio software program. The goal is set to have the highest gain and operating bandwidth possible. Only the diameter values are set to switchable and optimum values are determined as a result of this optimization process. The details of optimum antenna dimensions are shared in Table 1. As seen from the table, proposed antenna has an overall dimension of $1000 \times 1000 \times 100 \mu\text{m}^3$. It is also possible to define it in wavelength form for better comparison with other antenna studies as $0.33\lambda \times 0.33\lambda \times 0.03\lambda$ (where λ is the wavelength at the lowest operating frequency). The equations that the values in Table 1 derived from are given below, where W_p, L_p and f_r states patch width, patch length and desired resonant frequency, respectively [39]. Moreover, ϵ_{reff} and T_{sub} represents effective dielectric constant and substrate thickness. The antenna design is started once the initial width (W_p) and length (L_p) parameters are determined from the given equations. Afterwards, an octagonal structure is created, the patch and radiator element are shifted to the left by O and finally a trapezoidal transmission line is introduced to enhance antenna performances. The values in Table 1 are determined to reach the optimum gain and bandwidth performance at the desired frequency. The details of basic antenna design are not provided, since the focus of this study

is the implementation of PSO algorithm to determine the diameters of air cylinders. During the optimization process, lower and upper bounds of air cylinders are set as 60 and 120 mm, respectively. The goal is set to have a gain value above 10 dBi and fractional bandwidth of minimum 100%. Swarm size, maximum number of iterations and maximum number of solver equations are selected as 30, 15 and 451, respectively. Moreover, Latin Hypercube distribution is selected as the choice of initial point set.

$$\epsilon_{reff} = \frac{\epsilon_r + 1}{2} + \frac{\epsilon_r - 1}{2} \left(1 + 12 \frac{T_{sub}}{W_p} \right)^{-0.5} \quad (1)$$

$$W_p = \frac{c}{2f_r} \sqrt{\frac{2}{\epsilon_r + 1}} \quad (2)$$

$$L_p = \frac{c}{2f_r \sqrt{\epsilon_{reff}}} - 0.824 T_{sub} \frac{(\epsilon_{reff} + 0.3) \left(\frac{W_p}{T_{sub}} + 0.264 \right)}{(\epsilon_{reff} - 0.258) \left(\frac{W_p}{T_{sub}} + 0.8 \right)} \quad (3)$$

$$T_{sub} = 0.0606 \frac{\lambda}{\sqrt{\epsilon_r}} \quad (4)$$

The evolution stages of the proposed antenna design are depicted in Fig. 2. As seen in Fig. 2, a planar octagonal shaped microstrip patch antenna is designed initially with the help of the above given classical equations of antenna theory. It is observed from the simulations that having a partial ground plane that has a length equal to the length of the feeding line (L2) provides an enhancement in the performance. Therefore, including Ant.-1 all the antennas in the evolution stages have the same partial ground plane. The impedance bandwidth ($S_{11} \leq -10$ dB) of the two main bands of Ant.-1 are 0.118 THz and 0.49 THz. This corresponds to a fractional bandwidth percentage of 45.9% and 34.3%, respectively. The resonant frequencies of these bands are at 0.232 THz and 1.214 THz. Trapezoidal feeding line is implemented afterwards to widen the bandwidth. As seen in Fig. 3, this not only has an effect on the first main band, but also reduces the initial frequency value of the second band, where $S_{11} \leq -10$ dB, to 0.792 THz. In the next evolution stages, Ant.-3 is formed by shifting the antenna element to left by 100 μ m (O) and Ant.-4 is designed by etching a longitudinal elliptical slot to the radiating patch. This longitudinal slot provides a better impedance matching (50 Ω). It results an increase in resonant frequency and an improvement in the θ -polarized radiation. The optimum dimensions of this slot (R_x and R_y) are determined in such a way that it fulfills the aforementioned features. Once the bandwidth and radiation performance of Ant.-4 is analyzed and compared with similar THz antenna studies, it can be said that even Ant.-4 itself can be presented as a study that contributes to the literature. Nevertheless, a MPBG substrate

structure, which is the main focus of this study, is employed in the last design stage and further enhancements are achieved. The two main band intervals, resonant frequencies and reflection coefficient (S_{11}) values at that frequencies are provided in Table 2. As seen from the table and Fig. 3, each evolution stage enhances the bandwidth performance of antenna. Moreover, proposed antenna with its MPBG substrate has the highest bandwidth in 0-2 THz interval which is more than 1.522 THz.

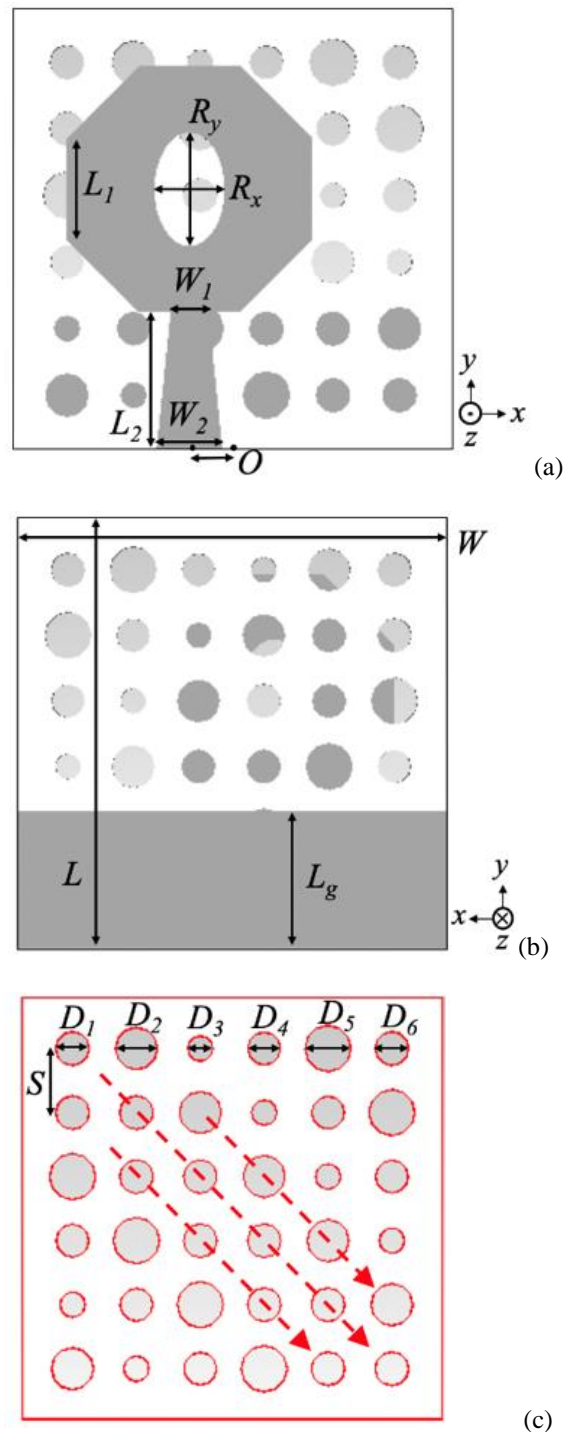


Figure 1. Antenna configuration (a) top view, (b) bottom view, (c) PBG substrate structure

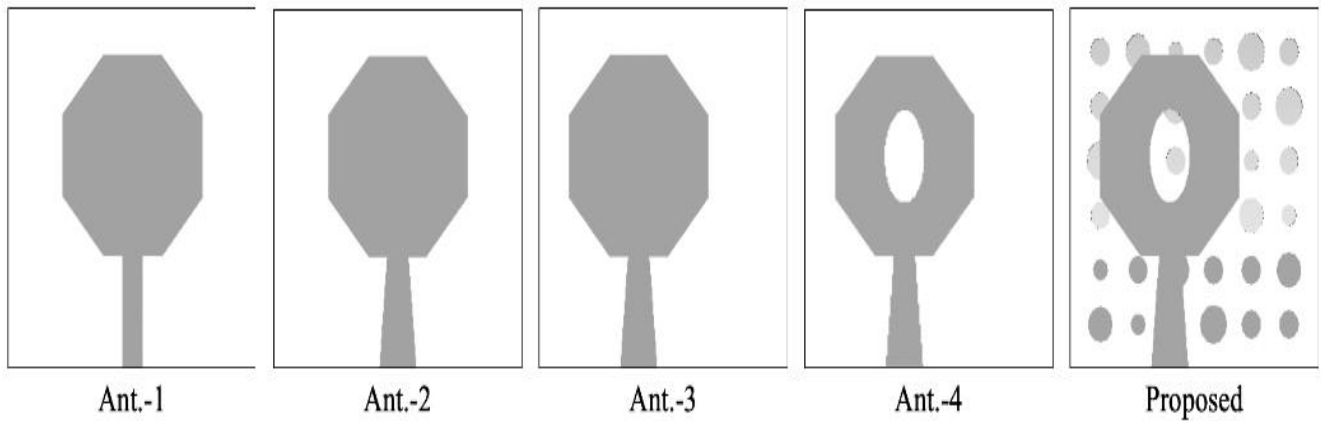


Figure 2. Evolution stages of the proposed antenna design

Table 1. Antenna layout dimensions

Parameter	W	L	D_1	D_2	D_3	D_4	D_5	D_6	S
Value (μm)	1000	1000	80	100	60	78	110	80	152
Parameter	L_1	L_2	W_1	W_2	R_x	R_y	L_g	O	
Value (μm)	230	320	86	150	80	130	320	100	

Table 2. The two main bands in 0-2 THz interval

Design	2 main bands (THz)	Bandwidth		Res. freq. (THz)	S_{11} (dB)
		(THz)	(%)		
Ant.-1	0.198-0.316	0.118	45.9	0.232	-14.53
	1.184-1.674	0.49	34.3	1.214	-43.53
Ant.-2	0.104-0.298	0.194	96.5	0.236	-20.36
	0.792-2	1.208	86.5	1.324	-33.39
Ant.-3	0.1-0.358	0.258	112.6	0.252	-22.98
	0.886-2	1.114	77.2	1.324	-31.79
Ant.-4	0.1-0.358	0.258	112.6	0.25	-23.18
	0.8-2	1.2	85.7	1.99	-42.11
Proposed	0.1-0.4	0.3	120	0.274	-19.41
	0.778-2	1.222	88	1.93	-38.82

3 Simulation results

Up until this section, the proposed antenna structure is discussed. The simulation results performed by using CST Microwave Studio [40] are analyzed in detail under this title by comparing the performance of the proposed design with different PBG structures. It is also important to emphasize that the antenna is electrically large in THz spectrum. This substantially increases the number of mesh cells and results in as computational complexity, which is one of the major difficulties faced throughout the simulation process.

Microstrip patch antennas are preferred frequently regardless of their operating frequency. These antennas have simple radiation characteristics that are common knowledge. Fringing fields constitute the primary source for the radiation of microstrip patch antennas. The amount of these fields is mainly dependent on the thickness and dielectric constant of the substrate material. Low dielectric constant results an enhancement in the fringing fields and radiation performance [29]. This enables the antenna to have high bandwidth, gain and directivity features.

THz antennas generally have thin substrates due to their minimized forms. However, thick substrate with a low dielectric constant is necessary for a desired radiation performance. Hence the reason why metamaterials have been used in some of the previous antenna studies to reduce the refractive index of the substrate material and to decrease the permittivity and permeability values. But unfortunately, metamaterials might not be very functional for THz antennas as these antennas have nanoscale structures [34]. Periodic air cavity substrate structures are developed as a solution, which results the formation of PBG in the dielectric substrate. Photonic crystals help to lower the dielectric constant of the antenna. They reduce the amount of accumulation of fields within the substrate and improve the radiation performance.

Another parameter that has an effect on the dielectric constant value of PBG structures is the lattice factor, which is defined as the ratio of air cylinder radius (R) to the distance between cylinders (S) [29]. Lattice factor value is optimized in this study to achieve the maximum gain value for the conventional PBG antenna structure. As seen in Fig. 4, an increase in lattice factor does not always result in an increase in realized gain. 8.03 is the highest gain value for conventional PBG antenna and this value is obtained when lattice value is 0.25. Therefore; R and S values are taken as 28 μm and 104 μm , respectively to meet the 0.25 lattice factor value.

The proposed antenna with MPBG substrate uses variable radii of air cylinders. The minimum and maximum values of these radii are 30 μm and 55 μm , respectively. The distance between air cylinders is 152 μm , so the lattice factor for MPBG structure varies from 0.197 to 0.362. The details of the proposed MPBG structure were given in the previous section.

Fig. 5 (a) depicts the frequency versus reflection coefficient (S11) graph of four different antenna structures that are: 1) an antenna without a PBG structure (Ant.-4), 2) an antenna with a conventional PBG substrate (R=28 μm ,

S=104 μm), 3) the proposed antenna with MPBG substrate and 4) an antenna with a surrounding MPBG structure. In the former antenna type, only the surrounding photonic air cylinders are utilized. Table 3 is created to summarize the bandwidth, gain and efficiency simulation results. As seen in Table 3, all the simulated antenna structures have two bands throughout the 0-2 THz interval, except conventional PBG antenna. Conventional PBG antenna has three bands and it offers one of the highest bandwidths in the first band with the proposed MPBG antenna. On the other hand, the conventional PBG structure has relatively narrow bandwidths in the rest of the two bands. The proposed antenna has the highest bandwidth within the 0-2 THz interval, which is 1.522 THz. Its bandwidth in the first and second bands are 0.3 THz and 1.222 THz, respectively. This correspond to the fractional bandwidth percentage of 120% and 88%, respectively. In comparison to the antenna without PBG, the reported design provides 8% and 11% improvement in the fractional bandwidth percentage for first and second bands, respectively.

Fig. 5(b) represents gain and efficiency results of all four antennas. The antenna without a PBG substrate has the lowest gain and efficiency values; whereas, the proposed MPBG antenna structure has the highest gain and efficiency values within the operating frequency range. The proposed design provides almost 300% gain improvement in comparison to the antenna without PBG. To the best of authors' knowledge, one of the highest gain enhancements is achieved with this study when the proposed technique is applied to the base antenna structure without PBG. Furthermore, both conventional PBG and surrounding MPBG substrate structures provide nearly the same values that are higher than the antenna without PBG, but lower than the proposed MPBG antenna structure. To summarize, although conventional PBG structure improves the radiation performance, it can further be improved by applying the proposed MPBG substrate structure.

The presented MPBG substrate structure is implemented to different substrate materials in Fig. 6. RT5880 has a lower dielectric constant ($\epsilon_r=2.2$), whereas glass ($\epsilon_r=6$) and RO3010 ($\epsilon_r=11.2$) have higher values in comparison to the RO4350B ($\epsilon_r=3.66$) substrate material that the proposed design is printed on. As discussed in the previous section, high permittivity dielectric substrate is not a desired feature for THz antennas. Hence, the result with RO3010 exhibits very narrow bands. Another important observation is that, although RT5880 has a lower dielectric constant, it does not offer a higher bandwidth. S11 value rises above -10 dB at 0.223 THz due to the design of the radiating patch. Moreover, the second band of the proposed antenna starts at 0.778 THz; whereas it starts at 1 THz for RT5880. As a result, the best performance is obtained with the proposed RO4350B material.

Radiation pattern of the antenna should also be analyzed to fully examine its radiation characteristic. 0.272 THz, 1.35 THz and 1.93 THz are the three resonant frequencies of the antenna; and Fig. 7 depicts the simulated far field radiation pattern of the proposed antenna at these resonant frequencies

in polar form. As seen from the figure, the E-plane (xz-plane) and H-plane (yz-plane) fields of the antenna has omnidirectional radiation properties at 0.272 and 1.93 THz. Besides that, the number of sidelobes increase considerably at higher frequencies. The co-polarized field in H-plane has a very directional pattern at 1.35 THz with low sidelobes and a directivity value of 10.8 dBi. It also has a wide half power beam width (HPBW) of 58°. This directional radiation feature has enabled the antenna to have a very high gain at 1.35 GHz frequency.

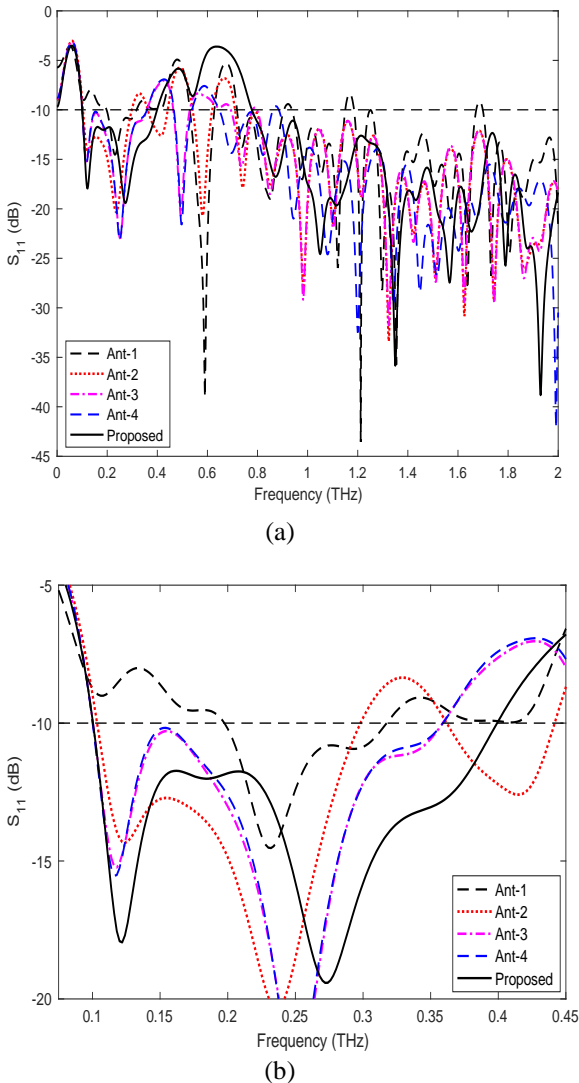


Figure 3. Effect of antenna evolution on reflection coefficient (a) for 0-2 THz interval and (b) in the first main band.

The proposed MPBG antenna structure is compared in Table 4 with some other state-of-art PBG THz antennas to verify the success of its radiation performance. All the studies presented in the comparison table have PBG substrates, but some are implemented in different form. It is easy to say that the proposed antenna with its MPBG substrate structure exhibits the highest gain value by far. Except from the study in [22], it also has the best radiation efficiency performance. Bandwidth is another important

parameter for most of the antenna designs, and it needs to be compared independent on frequency for a fair comparison. Therefore, fractional bandwidth values are calculated for each study. The reported design has the highest fractional bandwidth percentage values for both bands.

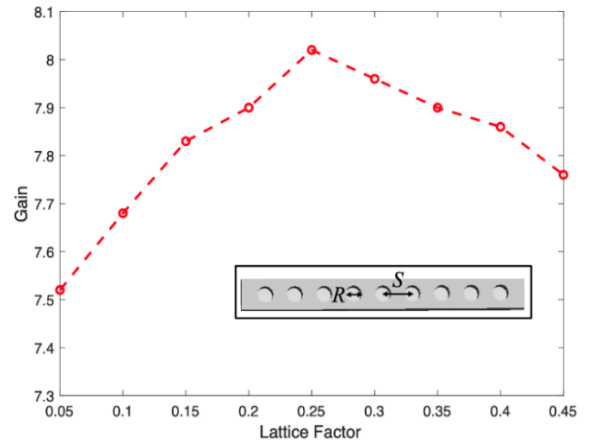


Figure 4. The effect of lattice factor on realized gain value of conventional PBG antenna at 1.3 THz.

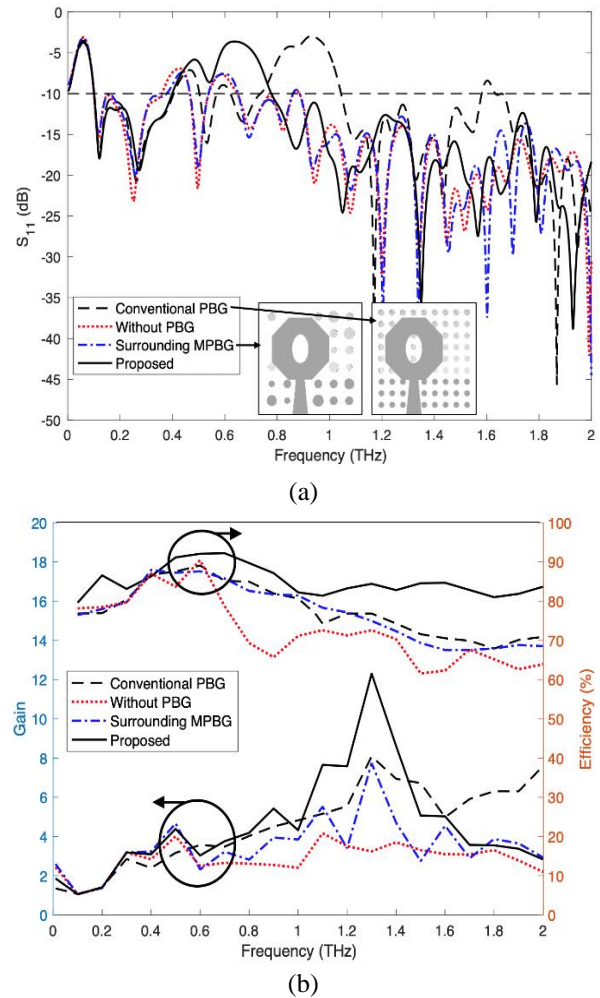


Figure 5. The effect of different substrate structure on antenna (a) bandwidth, (b) gain and efficiency

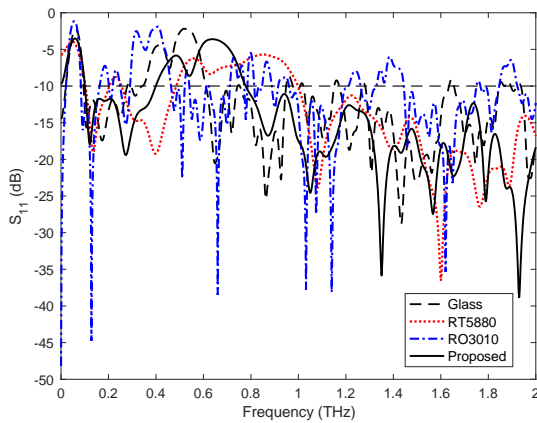


Figure 6. The effect of different substrate material on S_{11}

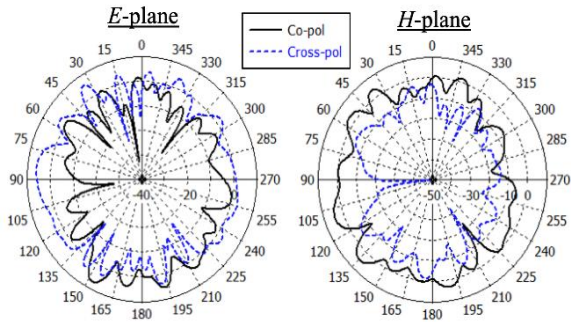
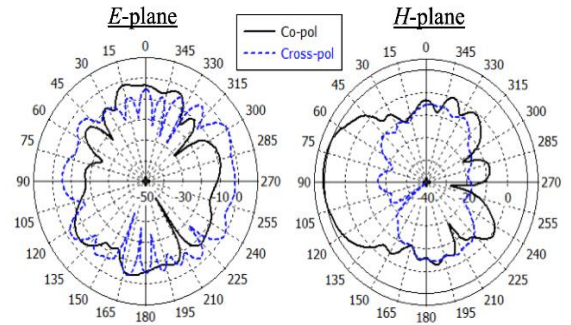
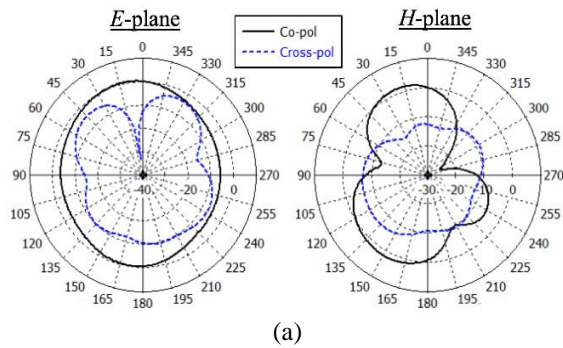


Figure 7. Far field radiation pattern of the proposed antenna structure for E-plane and H-plane at (a) 0.272 THz, (b) 1.35 THz and (c) 1.93 THz

Table 3. Bandwidth, gain and efficiency simulation results

Design	Main Bands (THz)	Bandwidth		Max. Realized Gain	Max. Efficiency (%)
		(THz)	(%)		
Without PBG (Ant.-4)	0.1-0.358	0.258	112	4.17 (@1.1 THz)	83.33 (@0.358 THz)
	0.888-2	1.112	77		
Conventional PBG	0.1-0.404	0.304	120.6	8.03 (@1.3 THz)	87.02 (@0.404 THz)
	1.044-1.58	0.536	40.9		
Surrounding MPBG	0.1-0.378	0.278	16.3	7.74 (@1.3 GHz)	86.21 (@0.378 THz)
	0.886-2	1.114	77.2		
Proposed	0.1-0.4	0.3	120	12.3 (@1.3 THz)	90.33 (@0.778 THz)
	0.778-2	1.222	88		

Table 4. Comparison with other THz studies available in literature

Study	Bandwidth (THz)	Bandwidth (%)	Max. Gain	Max. Efficiency (%)	Substrate Form
[20]	0.742	59.3	11	N.A.	Surrounding PBG
[21]	≈ 0.03	≈ 4.35	6.79	N.A.	Aperiodic PBG
[22]	0.128	21.2	9.17	91.08	Modified PBG
[23]	≈ 0.09	≈ 3.34	5	62	Quadratic hole PBG
[25]	≈ 0.265	34.3	8.45	88.3	Conventional PBG
[27]	0.3	14	4.97	79.62	Conventional PBG
[31]	≈ 0.35	≈ 66.66	9	88.72	Variable sized PBG
Proposed	0.3	120	12.3	90.33	Variable sized PBG (MPBG)
	1.222	88			

4 Conclusions

In this study, variable sized air cylinder cavities are implemented to the dielectric substrate to form a modified PBG substrate structure. Unlike conventional PBG structure, the diameter values of these cylinders are not the same throughout the substrate and they are determined to provide the highest gain and bandwidth values possible. PSO algorithm is used to assign the optimum values. The evolution stages and their positive effects on antenna bandwidth, gain and efficiency are analyzed. Moreover, the presented MPBG structure brings the antenna an almost 300% enhancement in gain and 8 to 11% improvement in fractional bandwidth percentage in comparison to the antenna without PBG. It is observed that the proposed MPBG THz antenna achieves an excellent radiation performance within a wide operating bandwidth.

Similarity rate (iThenticate): %5

Declaration of Competing Interest

The authors declare that they have no known competing financial interests or personal relationships that could have appeared to influence the work reported in this paper.

References

- [1] I. Malhotra, KR. Jha and G. Singh, Analysis of highly directive photoconductive dipole antenna at terahertz frequency for sensing and imaging applications. *Optics Communications*,397, 129-139, 2017. <https://doi.org/10.1016/j.optcom.2017.04.008>
- [2] A. El-Fatimy, JC. Delagnes, A. Younus, E. Nguema, F. Teppe, W. Knap, E. Abraham and P. Mounaix, Plasma wave field effect transistor as a resonant detector for 1 terahertz imaging applications. *Optics Communications*, 282(15), 3055-3058, 2009. <https://doi.org/10.1016/j.optcom.2009.04.054>
- [3] G. Geetharamani and T. Aathmanesan, Split ring resonator inspired THz antenna for breast cancer detection. *Optics & Laser Technology*,126, 106111, 2020. <https://doi.org/10.1016/j.optlastec.2020.106111>
- [4] S. Asgari, N. Granpayeh and T. Fabritius, Controllable terahertz cross-shaped three-dimensional graphene intrinsically chiral metastructure and its biosensing application. *Optics Communications*,474, 126080, 2020. <https://doi.org/10.1016/j.optcom.2020.126080>
- [5] R. Zhang, K. Yang, QH. Abbasi, KA. Qaraqe and A. Alomainy, Analytical modelling of the effect of noise on the terahertz in-vivo communication channel for body-centric nano-networks. *Nano Communication Networks*, 15, 59-68, 2018.<https://doi.org/10.1016/j.nancom.2017.04.001>
- [6] T. Okan, High efficiency unslotted ultra-wideband microstrip antenna for sub-terahertz short range wireless communication systems. *Optik*, 242, 166859, 2021. <https://doi.org/10.1016/j.ijleo.2021.166859>
- [7] KR. Jha and G. Singh, Design of highly directive cavity type terahertz antenna for wireless communication. *Optics Communications*,284 (20), 4996-5002, 2011. <https://doi.org/10.1016/j.optcom.2011.06.052>
- [8] X. Ma, Z. Chen, W. Chen, Y. Chi, Z. Li, C. Han and Q. Wen, Intelligent reflecting surface enhanced indoor terahertz communication systems. *Nano Communication Networks*, 24, 100284, 2020. <https://doi.org/10.1016/j.nancom.2020.100284>
- [9] T. Nagatsuma, K. Oogimoto, Y. Inubushi and J. Hirokawa, Practical considerations of terahertz communications for short distance applications. *Nano Communication Networks*, 10,1-12, 2016. <https://doi.org/10.1016/j.nancom.2016.07.005>
- [10] Q. Rubani, SH. Gupta, S. Pani and A. Kumar, Design and Analysis of a Terahertz Antenna for Wireless Body Area Networks. *Optik*, 179, 684-690, 2018. <https://doi.org/10.1016/j.ijleo.2018.10.202>
- [11] IF. Akyildiz, JM. Jornet and C. Han, Terahertz band: next frontier for wireless communications. *Physical Communication*, 12, 16-32, 2014. <https://doi.org/10.1016/j.phycom.2014.01.006>
- [12] FR. Yang, Y. Qian, R. Coccioli and T. Itoh, Analysis and Application of Photonic Band-Gap (PBG) Structures for Microwave Circuits. *Electromagnetics*, 19 (3), 241-254, 1999. [10.1080/02726349908908642](https://doi.org/10.1080/02726349908908642)
- [13] B. Dokmetas, GO. Arican, N. Akcam and E. Yazgan E, A novel millimeter-wave U-shaped radiating slot antenna with DGS structures for 5G cellular application. In: *IEEE, 11th International Conference on Electrical and Electronics Engineering (ELECO)*, Bursa, Turkey, pp: 669-672 28-30 November 2019. <https://doi.org/10.23919/ELECO47770.2019.8990502>
- [14] S. Singhal S, Four Arm Windmill Shaped Superwideband Terahertz MIMO Fractal Antenna. *Optik*, 219, 165093, 2020. <https://doi.org/10.1016/j.ijleo.2020.165093>
- [15] MG. Silveirinha and CA. Fernandes, Computation of the Electromagnetic Modes in Two-Dimensional Photonic Crystals: A Technique to Improve the Convergence Rate of the Plane Wave Method. *Electromagnetics*. 26 (2), 175-187, 2006. <https://doi.org/10.1080/02726340500486492>
- [16] A. Sharma and G. Singh, Rectangular Microstrip Patch Antenna Design at THz Frequency for Short Distance Wireless Communication Systems. *Journal of Infrared, Millimeter, and Terahertz Waves*, 30 (1), 1-7, 2008.
- [17] Á. Gómez, A. Vegas, MA. Solano and A. Lakhtakia On One- and Two-Dimensional Electromagnetic Band Gap Structures in Rectangular Waveguides. *Microwave Frequencies. Electromagnetics*, 25(5), 437-460, 2005. <https://doi.org/10.1080/02726340590957443>
- [18] M. Singh and S. Singh, Design and Performance Investigation of Miniaturized Multi-Wideband Patch Antenna for Multiple Terahertz Applications. *Photonics and Nanostructures-Fundamentals and Applications*, 44,100900, 2021 <https://doi.org/10.1016/j.photonics.2021.100900>

- [19] TS. Rappaport, Y. Xing, O. Kanhere, S. Ju, A. Madanayake, S. Mandal, A. Alkhateeb and GC. Trichopoulos, Wireless Communications and Applications Above 100 GHz: Opportunities and Challenges for 6G and Beyond. *IEEE Access*. 7,78729-78757, 2019. <https://doi.org/10.1109/ACCESS.2019.2921522>
- [20] A. Singh and S. Singh, A trapezoidal microstrip patch antenna on photonic crystal substrate for high speed THz applications. *Photonics and Nanostructures - Fundamentals and Applications*,14, 52-62, 2015. <https://doi.org/10.1016/j.photonics.2015.01.003>
- [21] S. Ullah, C. Ruan, TU. Haq and X. Zhang, High performance THz patch antenna using photonic band gap and defected ground structure. *Journal of Electromagnetic Waves and Applications*, 33 (15), 1943-1954, 2019. <https://doi.org/10.1080/09205071.2019.1654929>
- [22] MNE. Temmar, A. Hocini, D. Khedrouche and M. Zamani, Analysis and design of a terahertz microstrip antenna based on a synthesized photonic bandgap substrate using BPSO. *Journal of Computational Electronics*, 18, 231-240, 2019.
- [23] BO. De Andrade and LM. De Mendonca, Frequency invariance, gain improvement, and fast design in 3D-printed photonic band gap antennas with quadratic holes. *Microwave and Optical Technology Letters*. 61 (10), 2295-2305, 2019. <https://doi.org/10.1002/mop.31897>
- [24] JPP. Pereira, JP. Da Silva and HD. De Andrade, A new design and analysis of a hexagonal PBG microstrip antenna. *Microwave and Optical Technology Letters*, 57 (9), 2147-2151, 2015. <https://doi.org/10.1002/mop.29279>
- [25] G. Singh, Design considerations for rectangular microstrip patch antenna on electromagnetic crystal substrate at terahertz frequency. *Infrared Physics & Technology*, 53 (1), 17-22, 2010. <https://doi.org/10.1016/j.infrared.2009.08.002>
- [26] MN. Eddine-Temmar, A. Hocini, D. Khedrouche and TA. Denidni, Analysis and Design of MIMO Indoor Communication System Using Terahertz Patch Antenna Based on Photonic Crystal with Graphene. *Photonics and Nanostructures - Fundamentals and Applications*, 43,100867, 2020. <https://doi.org/10.1016/j.photonics.2020.100867>
- [27] S. Anand, DS. Kumar, RJ. Wu and M. Chavali, Analysis and design of optically transparent antenna on photonic band gap structures. *Optik*,125 (12), 2835-2839, 2014. <https://doi.org/10.1016/j.ijleo.2013.11.061>
- [28] E. Rahmati and M. Ahmadi-Boroujeni, Improving the efficiency and directivity of THz photoconductive antennas by using a defective photonic crystal substrate. *Optics Communications*, 412, 74-79, 2018. <https://doi.org/10.1016/j.optcom.2017.12.011>
- [29] KR. Jha and G. Singh, Analysis and design of terahertz microstrip antenna on photonic bandgap material. *Journal of Computational Electronics*, 11 (4), 364-373, 2012.
- [30] MN. Eddine-Temmar, A. Hocini, D. Khedrouche and TA. Denidni, Enhanced Flexible Terahertz Microstrip Antenna Based on Modified Silicon-Air Photonic Crystal. *Optik*, 217, 164897, 2020. <https://doi.org/10.1016/j.ijleo.2020.164897>
- [31] A. Hocini, MN. Temmar, D. Khedrouche and M. Zamani, Novel Approach for the Design and Analysis of a Terahertz Microstrip Patch Antenna Based on Photonic Crystals. *Photonics and Nanostructures - Fundamentals and Applications*,36,100723,2019. <https://doi.org/10.1016/j.photonics.2019.100723>
- [32] MS. Khan, AD. Capobianco, SM. Asif, A. Iftikhar, BD. Braaten and RM. Shubair, A properties comparison between copper and graphene-based UWB MIMO planar antennas. In: *IEEE, International Symposium on Antennas and Propagation (APSURSI), Puerto Rico; 26 June-1 July 2016:1767-1768*. <https://doi.org/10.1109/APS.2016.7696590>
- [33] T. Zhou, Z. Cheng, H. Zhang, M. Le Berre, L. Militaru and F. Calmon, Miniaturized tunable terahertz antenna based on graphene. *Microwave and Optical Technology Letters*, 56 (8), 1792-1794, 2014. <https://doi.org/10.1002/mop.28450>
- [34] R. Goyal R and DK. Vishwakarma, Design of a graphene-based patch antenna on glass substrate for high-speed terahertz communications. *Microwave and Optical Technology Letters*, 60 (7), 1594-1600, 2018. <https://doi.org/10.1002/mop.31216>
- [35] JY. Liu, TJ. Huang, FY. Han, LZ. Yin and PK. Liu, Terahertz routing with graphene magnetic metamaterials. *Optics Communications*, 464, 125506, 2020. <https://doi.org/10.1016/j.optcom.2020.125506>
- [36] P. Upende and A. Kumar, Quad-Band Circularly Polarized Tunable Graphene Based Dielectric Resonator Antenna for Terahertz Applications. *Silicon*, 2021.
- [37] CM. Krishna, S. Das, S. Lakrit, S. Lavadiya, BTP. Madhav and V. Sorathiya, Design and analysis of a super wideband (0.09-30.14 THz) graphene based log periodic dipole array antenna for terahertz applications. *Optik*, 247, 167991, 2021. <https://doi.org/10.1016/j.ijleo.2021.167991>
- [38] AE. Yilmaz and M. Kuzuoglu, Calculation of optimized parameters of rectangular microstrip patch antenna using particle swarm optimization. *Microwave and Optical Technology Letters*, 49 (12), 2905-2907, 2007. <https://doi.org/10.1002/mop.22918>
- [39] CA. Balanis, *Antenna theory: analysis and design*. 3rd ed. New York, J. Wiley, 2005.
- [40] CST Microwave Studio Suite, CST Inc.; 2018.

